Design and Analysis of a High Performance Impedance Based Hybrid Haptic Interface

Patrick Dills, Chembian Parthiban, It Fufuengsin, and Michael Zinn, *Member, IEEE*

***Abstract*— This paper describes the design of a novel, high-performance one degree-of-freedom hybrid haptic interface. The interface integrates a particle brake, a Series Elastic Actuator (SEA), and a small DC motor into a single actuator. Unlike existing hybrid designs, the one presented here does not suffer from a significant mismatch between passive and active torque capability. The paper describes the design of the three actuator components. The motivation for selecting a particle brake is discussed. The SEA design approach is contextualized through its integration into the hybrid actuator, and the ideal SEA spring stiffness for the actuator is explored. Finally, mini motor design and sizing considering SEA and particle brake performance is included. The interface design provides insight into the dynamics of the system as a whole and allows for additional future work in control and optimization.**

I. Introduction

The majority of haptic interfaces are active interfaces utilizing impedance—based control and EM motors. Impedance based devices have limitations on their rendering range due to encoder quantization [1], device compliance [2], and other sources. Colgate and Brown showed the Z-width, or range of achievable impedances, is increased by adding physical damping to the system. This insight lead to interest in passive actuators used as active dampers in conjunction with active EM motors to increase the rendering range of the entire device [3]. Other advantages of hybrid haptics include increased energy efficiency, as shown with the H2O actuation approach [4], and increased torque density. While these hybrid actuators show clear improvements, the passive elements of the hybrid actuators are heavily nonlinear, making control challenging. In addition, existing hybrid devices often suffer from significant mismatch between passive and active torque capability, complicating the control and affecting the rendering performance [5].

This paper describes the design and development of a high—performance desktop hybrid haptic interface. The device is meant to provide a platform to explore control and estimation strategies to maximize performance, z-width, while remaining safe and robust.

II. Hybrid Testbed Motivation and Overview

The hybrid haptic testbed must be able to display active and passive torques over a large frequency range. In addition, the device must maintain low output impedance for device transparency. To achieve this, the hybrid haptic interface is comprised of a low frequency passive actuator (particle brake), a low-frequency active actuator (series elastic actuator), and a high-frequency active actuator (mini) arranged in parallel. The combined system has low output impedance and high-bandwidth torque response. Unlike other hybrid actuators, the system described here will not suffer from a large relative asymmetry of passive and active torques, a limitation of current hybrid approaches. The following sections describe the motivation and design of each of these elements.

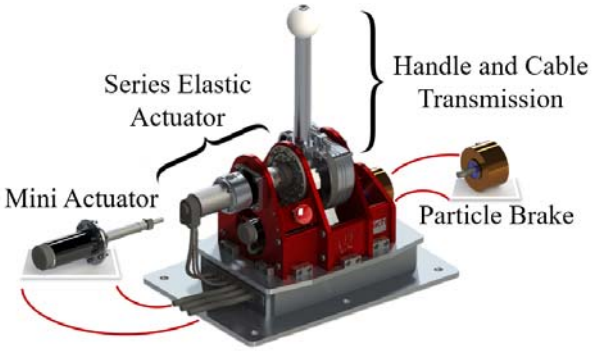

Figure 1. Hybrid testbed overview, mini motor and particle brake.

III. Passive Actuator: Particle Brake

A particle brake (see Figure 1) has been selected as the interface's passive actuator. Particle brake selection is motivated by attaining the fastest response possible while minimizing nonlinear characteristics typically associated with passive actuators. To minimize response time while limiting the reflected inertia of the brake, a low reduction (11:1) single-stage cable reducer is placed between the brake and output shaft. The use of a cable reduction minimizes the resulting friction while allowing for use of a smaller brake, thus decreasing the response time while maintaining high torque density and low rotor inertia, for improved transparency. Advantages of particle brakes over other passive actuators include, smooth torque operation (hysteresis brakes have cogging torque), zero velocity torque output (eddy current brake torque is zero at zero velocity), and commercial availability in many sizes (MR and ER brakes are mostly custom designs).

IV. Series Elastic Actuator

A Series Elastic Actuator (SEA) provides the low frequency active torque component of the hybrid testbed while maintaining low output impedance [6].

Patrick Dills, Chembian Parthiban, It Fufuengsin and Michael Zinn are with the Department of Mechanical Engineering, University of Wisconsin - Madison (e-mail: pdills|parthiban|fufuengsin|mike.zinn@wisc.edu)

A. Closed-loop bandwidth

The performance of a SEA is directly related to the closed loop bandwidth of its torque controller. To maximize the bandwidth our SEA design utilizes a low inertia brushless DC motor, a zero backlash harmonic drive, and a single analog sensor measurement for the feedback signal to maximize the closed loop bandwidth [7]. A higher closed loop bandwidth results in a lower output impedance over a larger frequency range and an improved actuator.

B. SEA spring stiffness

The SEA spring stiffness has a direct impact on the stability and performance of the actuator. As part of the control and estimation effort, a range of spring stiffness are considered, Table 2. The most compliant spring considered is limited by practical considerations such as the maximum allowable deflection and the needed output torque (6.47 [Nm/rad]). The maximum stiffness is limited by the maximum SEA bandwidth, and effects both the actuators large signal bandwidth, and the actuators high frequency output impedance.

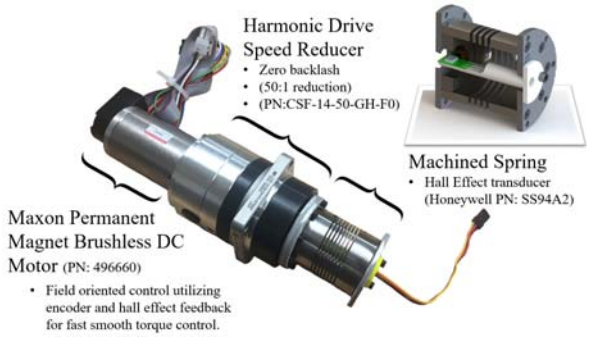

Figure 2. Completed SEA with section view of the elastic element.

C. Maximum Spring Stiffness

To maintain a robust controller, the open loop natural frequency of the SEA should be designed below the controller's bandwidth [2]. While the natural frequency varies with the drive load inertia, we can bracket the expected values by considering, free space operation and fixed load operation. Depending on the inertia of the load and the motor, the highest natural frequency may change and should be used to establish the upper limit of SEA spring stiffness. Equations (1) and (2), fixed and free operation respectively, define guidelines for the upper limit of the SEA open loop natural frequency.

$$\omega_{nfixed} = \sqrt{\frac{K_{sp}}{J_{meq}}} \leq \frac{\omega_{bwSEA}}{N} \tag{1}$$

$$\omega_{nfree} = \sqrt{\frac{K_{sp}\left(J_{meq}+J_{leq}\right)}{\left(J_{meq}J_{leq}\right)}} \leq \frac{\omega_{bwSEA}}{N} \tag{2}$$

where: $N =$ Bandwidth Factor of Safety

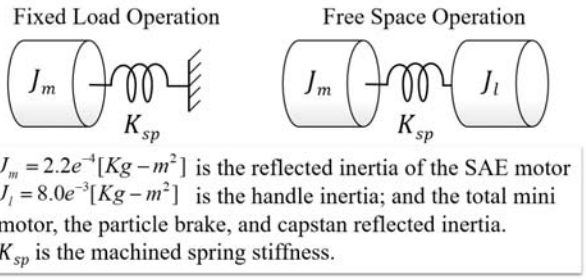

Figure 3. SEA lumped parameter models.

For the haptic interface described here, the resulting undamped natural frequencies and resulting maximum spring stiffness are shown in Table 1.

Table 1— SEA limitation on maximum spring stiffness.

(N=3, ω_{bw}=30Hz)		**Maximum Stiffness [Nm/rad]**
$\omega_{n\ fixed}$ [Hz]	6.63	43.42
$\omega_{n\ free}$ [Hz]	10.00	19.14

Here the free space operating case is the most restrictive and will serve as the maximum spring value.

In addition to the closed loop bandwidth, the large signal (torque) bandwidth has a direct effect on the performance and stability of the haptic testbed [7]. The maximum available SEA output torque T_{lmax}, as a function of frequency (limited by actuator torque, T_{sat} and velocity saturation V_{sat}) is given by (3)

$$T_{l\max} = T_{sat}\left(\frac{\omega_0}{s+\omega_0}\right) \rightarrow \omega_0 = K_{sp}\frac{V_{sat}}{T_{sat}} \tag{3}$$

As seen from (3), the large signal bandwidth is directly proportional to the spring stiffness suggesting actuator performance improves with increased spring stiffness [7].

D. Minimum Spring Stiffness

The SEA must also interact and operate seamlessly as part of a hybrid actuator. To do so, the SEA must have a low output impedance above its control bandwidth to ensure the parallel operation of all three actuators. Using the simplified fixed load model shown in Figure 3, we can evaluate the closed loop impedance of the system as a function of frequency, (4).

$$\frac{T_l(s)}{\theta_l(s)} = \frac{-s^2 J_{meq}K_{sp}}{s^2 J_{meq} + K_{sp} + K_{sp}(K_p + sK_d)} \tag{4}$$

As seen in Figure 4 and (4) the output impedance above the closed loop bandwidth of the SEA is directly proportional to the spring's stiffness. While the optimal value of the stiffness is not known, it is clear that lowering spring stiffness will increase the effectiveness of the mini actuator by reducing the output impedance of the spring.

Table 2—Hybrid testbed SEA spring stiffness range.

(N=3, ω_{bw}=30Hz)	**Min. Stiffness**	**Max. Stiffness**
K_{sp} [Nm/rad]	6.47	19.14
$\omega_{n\ fixed}$ [Hz]	3.85	6.63
$\omega_{n\ free}$ [Hz]	5.81	10.00

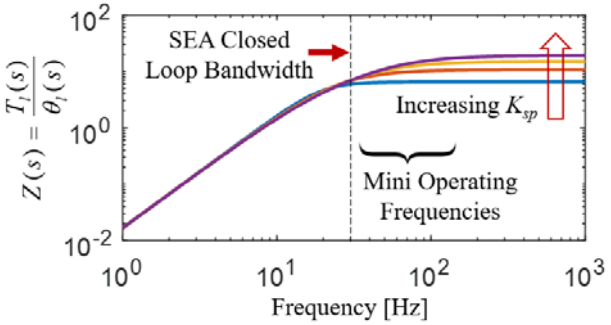

Figure 4. Closed loop output impedance of the testbed under fixed wall operation and the possible range of spring stiffness's. (K_p=25,K_d=0.3)

Figure 4 suggests that a lower spring stiffness may improve overall performance and is a subject of further investigation. Table 2 shows the range of spring stiffness's to be considered.

V. Mini Actuator

To provide high-frequency torque content, essential for high performance haptic rendering, our design includes a fast EM servo motor, referred to here as the mini. The incorporation of the mini is necessitated by the slow response of both the passive particle brake and active SEA. The brake selected for the hybrid testbed achieves a response time between 10 and 20 ms. The SEA, tuned to 30Hz bandwidth also has a response time of about 20ms. Neither actuator has the capability to produce the high frequency torque content needed to render stiff surfaces. A parallel mini motor with a quick response time and high instantaneous torque increases the maximum stiffness the hybrid actuator can produce. The selected mini motor is a Maxon ironless core brushed DC motor with a quick response time, a low rotor inertia, no cogging torque, and low torque ripple. To increase the torque density of the mini, a low reduction (11:1) single-stage cable reducer is placed between the mini and output shaft. The use of a cable reduction minimizes the resulting friction while increasing the torque density.

The performance of the mini-actuator is limited by its thermal response (winding temperature) which is directly related to its torque profile. While the actual mini torque profile depends on many things the profile shown in Figure 6 represents a conservative case where the hybrid actuator torque profile is switched between its maximum output torque and zero continuously with a 50% duty cycle. The mini actuator must supply the transient (high frequency) torque the SEA and/or particle brake cannot.

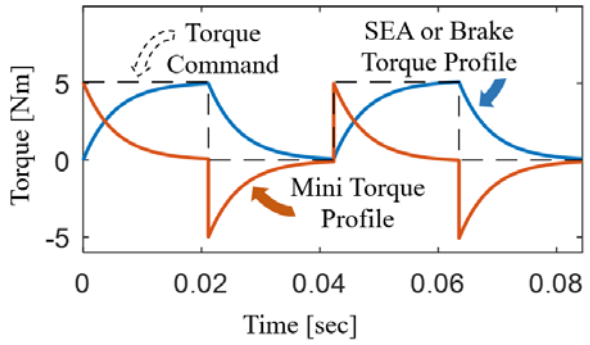

Figure 5. Ideal time response of low frequency actuator and mini motor to a square wave command.

To evaluate the winding temperature, we use a lumped parameter thermal model (see Figure 6) to evaluate the steady-state maximum winding temperature due to the continuous application of the switching torque signal (Figure 5). For the DC motor selected, thermal analysis shows that the maximum torque switching frequency where the winding temperature remains below its maximum limit of 155[C] is 23 Hz. This frequency is above the expected human interaction frequency, less than 5 Hz, and shows the mini motor will be able to provide the needed high frequency torque without winding failures.

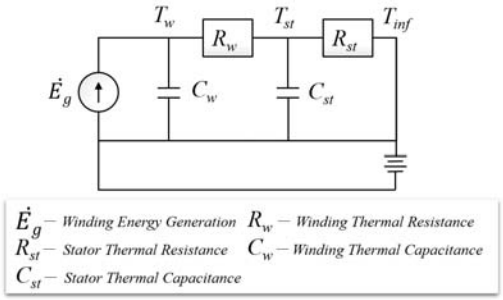

Figure 6. Lumped parameter thermal model of the mini motor

VI. Conclusion

We have described the design and supporting analysis of a high-performance hybrid haptic interface comprised of a low frequency passive actuator (particle brake), a low-frequency active actuator (SEA), and a high-frequency active actuator (mini). The combined system will have low output impedance and high-bandwidth torque response. Unlike other hybrid actuators, the system described here will not suffer from a large relative asymmetry of passive and active torques, a limitation of current hybrid approaches. The testbed will provide opportunities to further investigate control and estimation strategies, improving hybrid haptic actuators in the future

References

[1] J. E. Colgate and J. M. Brown, "Factors affecting the Z-Width of a haptic display," Proceedings of the 1994 IEEE International Conference on Robotics and Automation, San Diego, CA, 1994, pp. 3205-3210 vol.4.

[2] M. Zinn, O. Khatib, B. Roth and J. K. Salisbury, "Large Workspace Haptic Devices - A New Actuation Approach," 2008 Symposium on Haptic Interfaces for Virtual Environment and Teleoperator Systems, Reno, NE, 2008, pp. 185-192.

[3] J. An and D. Kwon, "In haptics, the influence of the controllable physical damping on stability and performance," 2004 IEEE/RSJ International Conference on Intelligent Robots and Systems (IROS) (IEEE Cat. No.04CH37566), 2004, pp. 1204-1209 vol.2.

[4] F.Conti and O.Khatib,"A New Actuation Approach for Haptic Interface Design", The International Journal of Robotics Research 2009;28 834-848.

[5] C. Rossa, J. Lozada and A. Micaelli, "Design and Control of a Dual Unidirectional Brake Hybrid Actuation System for Haptic Devices," in IEEE Transactions on Haptics, vol. 7, no. 4, pp. 442-453, Oct.-Dec. 1 2014.

[6] M. M. Williamson, 'Series Elastic Actuators," M.S Thesis, Dept. Computer Science and Electrical Engineering, Massachusetts Institute of Technology, Cambridge, MA,1995.

[7] D. W. Robinson, 'Design and Analysis of Series Elasticity in Closed-loop Actuator Force Control," Ph.D. dissertation, Dept. Mechanical Engineering, Massachusetts Institute of Technology, Cambridge, MA,1995.